# EPR and ENDOR Study of Trigonal Bipyramidal Copper Complexes with a Nitrogen Donor Tripodal Ligand

**Muhammad Q. Ehsan, Yasunori Ohba, Seigo Yamauchi, and Masamoto Iwaizumi***

Institute for Chemical Reaction Science, Tohoku University, Katahira 2-1-1, Aoba-ku, Sendai 980-77

(Received January 26, 1996)

The characteristic features of the electronic structure of some trigonal bipyramidal (tbp) copper complexes of the quadridentate tripodal nitrogen donor ligands, tris(2-aminoethyl)amine (tren) and tris(2-dimethylaminoethyl)amine (trenMe$_6$), with different ligands at the fifth coordination position of tbp were studied in a powder form doped in diamagnetic zinc complexes by EPR and ENDOR. EPR shows that the copper complexes of tren and trenMe$_6$ have a ground state with a $d_{z^2}$ unpaired electron orbital, and that some of the complexes are distorted from a trigonal symmetry to rhombic, to the contrary to expectations from the molecular formula. It is shown that a small structural or ligand-field distortion would give a recognizable spectral deviation from trigonal symmetry. It should be noticed that the hyperfine couplings of all the coordinating nitrogen atoms in each complex were observed by ENDOR, and that they were useful for calrifying the characteristic features of the electronic structures of the tbp complexes. The ligand fields at the fifth coordination position of tbp affects all of the coordination bonds as well as the spin distribution among the ligands. These ligand field effects on the electronic structures are discussed in reference to the ligand field parameters obtained by an EPR analysis. It is also shown that the ENDOR analysis well predicts the sp ratios of the coordinating orbitals of nitrogens, consistent with those obtained from the X-ray structural data on the complexes.

ENDOR spectroscopy has been effectively applied to investigations of the electronic structures of tetragonal copper(II) complexes. Especially, the method of angle-selected ENDOR[1] has been useful for structural studies of complexes in the disordered state, such as powder or frozen solution samples. However, there have been few investigations on copper(II) complexes having structures largely distorted from tetragonal or of trigonal symmetry by ENDOR.[1i,k] Some copper proteins have copper binding sites involving structures largely distorted from tetragonal symmetry. For example, it has been shown that some blue copper proteins have copper binding sites involving a trigonal pyramidal or trigonal bipyramidal coordination structure; a few ENDOR investigations have been published on these proteins.[2] However, it seems to be interesting to elucidate the characteristic features of the electronic structures of complexes having well-defined coordination structures, which are of largely distorted from tetragonal symmetry or of trigonal symmetry. In a previous communication we reported on the results obtained by ENDOR for trigonal bipyramidal (tbp) copper complexes of a nitrogen donor quadridentate tripodal ligand, tris(2-aminoethyl)amine (tren), with NCS and $NH_3$ at the fifth coordination position.[3] In the present paper we report on EPR and ENDOR studies concerning tbp complexes with tren and tris(dimethylaminoethyl)amine (trenMe$_6$) with different small ligands ($ClO_4^-$, $Cl^-$, $Br^-$, $I^-$, $NCS^-$, and $NH_3$) at the fifth position of tbp (Fig. 1). Recently, an ESEEM study on some tbp copper complexes with substituted imidazoles was reported.[4] In this paper, although the hyperfine coupling (HFC) and nuclear quadrupole coupling (NQC) constants of the remote nitrogen of the substituted imidazoles were determined, no direct information concerning the metal coordinating nitrogen bonds was given. In the present study, the HFC constants of all the nitrogens coordinated to copper were observed, and some characteristic features of the ground electronic structure of the complexes were clarified by EPR and ENDOR analyses.

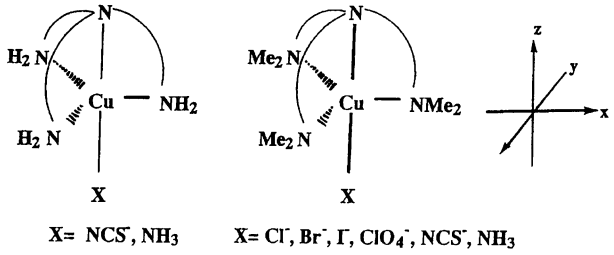


Fig. 1. Structures of tbp copper complexes of tren and trenMe$_6$.

## Experimental

**Materials.** The nitrogen donor tripodal ligand, tren, was commercially obtained from Wako Pure Chemical Industries Ltd. and used without purification. The ligand trenMe$_6$ was synthesized by methylation of tren according to the literature.[5] From these ligands the following complexes were prepared: [Cu(trenMe$_6$)ClO$_4$]ClO$_4$, **1**, (Found: C, 28.82; H, 6.31; N, 11.13; Cl, 14.98%. Calcd for $CuC_{12}H_{30}N_4O_8Cl_2$: C, 29.20; H, 6.08; N, 11.35; Cl, 14.40%), [Cu(trenMe$_6$)Br]Br, **2**, (Found: C, 31.90; H, 6.55; N, 12.27%. Calcd for $CuC_{12}H_{30}N_4Br_2$: C, 31.76; H, 6.66; N, 12.35%), [Cu(trenMe$_6$)I]ClO$_4$, **3**, (Found: C, 27.48; H, 5.64; N, 10.97; Hal, 31.61%. Calcd for $CuC_{12}H_{30}N_4O_4ICl$: C, 27.69; H, 5.81; N, 10.77; Hal, 31.20%),

[Cu(trenMe$_6$)Cl]ClO$_4$, **4**, (Found: C, 33.33; H, 6.90; N, 12.80; Cl, 16.06%. Calcd for $CuC_{12}H_{30}N_4O_4Cl_2$: C, 33.61; H, 7.05; N, 13.06; Cl, 16.53%), [Cu(trenMe$_6$)NCS]SCN, **5**, (Found: C, 40.21; H, 7.57; N, 20.22%. Calcd for $CuC_{14}H_{30}N_6S_2$: C, 41.02; H, 7.32; N, 20.50%), [Cu(trenMe$_6$)NH$_3$](ClO$_4$)$_2$, **6**, (Found: C, 28.18; H, 6.34; N, 13.80; Cl, 13.59%. Calcd for $CuC_{12}H_{33}N_5O_8Cl_2$: C, 28.26; H, 6.52; N, 13.74; Cl, 13.91%), [Cu(tren)NCS]SCN, **7**, (Found: C, 29.45; H, 5.52; N, 26.10%. Calcd for $CuC_8H_{18}N_6S_2$: C, 30.61; H, 5.78; N, 26.78%), and [Cu(tren)NH$_3$](ClO$_4$)$_2$, **8**, (Found: C, 16.98; H, 4.90; N, 16.42; Cl, 16.53%. Calcd for $CuC_6H_{12}N_5O_8Cl_2$: C, 17.42; H, 5.12; N, 16.94; Cl, 17.14%). For EPR and ENDOR measurements these complexes were doped in diamagnetic host crystals. For all of the complexes, the corresponding zinc complexes were used as host matrices for the geometrical similarity between the respective zinc and copper complexes. Doping was done by coprecipitation from the matrix complex solutions containing a 2—8% copper complex.

**Measurements of the EPR and ENDOR Spectra.** The powder EPR spectra of the complexes were recorded on a Varian E-112 EPR spectrometer equipped with an E-102 microwave (MW) bridge for X-band EPR measurements and with an E-110 MW bridge for Q-band EPR. The MW frequencies of the X-band experiments were read from a Takeda Riken TR 5204 frequency counter. The NMR field meter (EFM 2000 of Echo Electric company) was used to measure the magnetic field strength. Powder ENDOR spectra were recorded on the same EPR spectrometer equipped with a Varian E-1700 ENDOR unit using a Micro Device type MSC-10EB TE011 ENDOR cavity. The radiowave power was amplified by a 550L 50-Watt RF power amplifier from Electronic Navigation Industries. A laboratory-made variable-frequency/duty RF pulsing circuit was used for the RF modulator.

To distinguish the nitrogen and proton ENDOR signals, the ENDOR spectra were observed at two different MW frequencies. To change the MW frequencies, a small aluminum ring was inserted into the top of the ENDOR cavity; the increment of the resonance frequency by insertion of the aluminum piece was about 0.5 GHz. The proton and nitrogen ENDOR signals were also distinguished from each other by changing the doping level of paramagnetic species in the range of 1—8%. The change of the spin relaxation time by the doping level affects differently the ENDOR intensities for nitrogens and protons; at a high doping concentration (5—8%) the relative intensity of the nitrogens to that of protons increases, and at low concentration the trend is reversed. Deuteration of the $NH_2$ protons in the tren complexes was also useful for identifying the proton signals.

## Results and Discussion

**Analysis of the EPR Spectra.** Figure 2 shows an example of the X-band and Q-band EPR spectra of the tbp copper complexes and their simulation spectra. The points shown in the X-band EPR spectrum (a—g) indicate the magnetic field settings at which the ENDOR spectra were taken. All of the spectral patterns observed for the complexes show that $g_x, g_y > g_z \fallingdotseq 2$, indicating that the complexes have a ground state with an unpaired electron in the $d_{z^2}$ orbital.[6] Such a ground state results from ligand fields which are stronger in the axial direction than in the equatorial plane. The EPR parameters were determined by a computer simulation of the spectra. The simulations were performed using a computer program written on the basis of a second-order solution of the

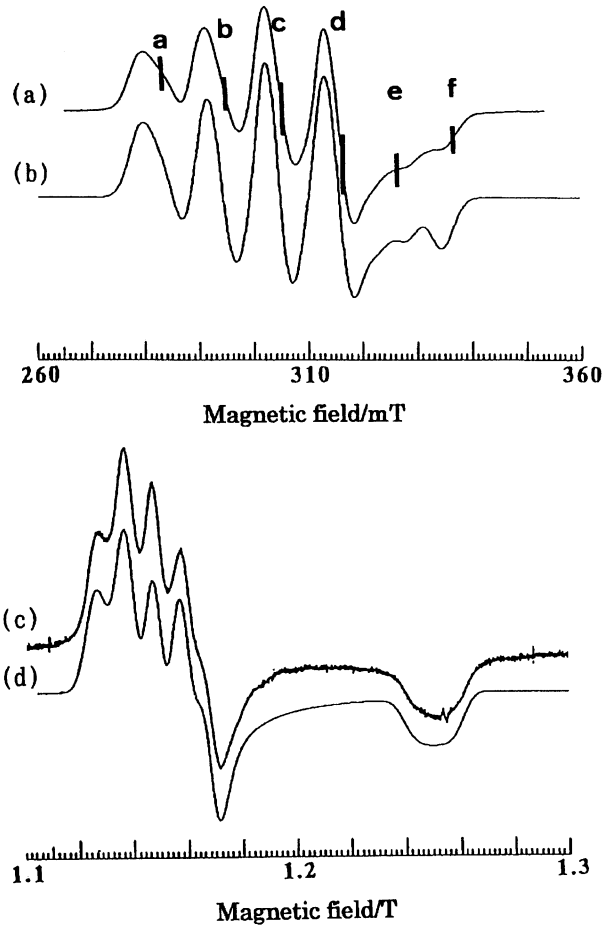


Fig. 2. Powder EPR spectra of [Cu(trenMe$_6$)NCS]SCN. a) X-band EPR spectrum recorded at 4.8 K and 9.1191 GHz MW frequency. b) Simulated X-band EPR spectrum by the g and Cu hfc constants in Table 1. c) Q-band EPR spectrum recorded at room temperature and 34.990 GHz MW frequency. d) Simulated Q-band EPR spectrum by the same $g$ and Cu hfc constants as in (b). The points a—g in the X-band EPR spectrum indicate magnetic set positions at which ENDOR spectra were observed.

spin Hamiltonian, including the electron Zeeman and copper HFC interactions in an arbitary coordinate system, according to Iwasaki.[7] The presence of copper isotopes, line-width anisotropies and forbidden transitions were also taken into consideration. A Gaussian function was used for the line shape. The obtained EPR parameters are listed in Table 1. It is notable that, as is seen from the spectra of Fig. 1, some complexes are distorted to rhombic symmetry, which is contrary to the expectation from the molecular formula. We consider the rhombicity of the spectra in the following.

**Rhombicity in the EPR Spectra.** As a general case of copper complexes with rhombic distortion, we express the unpaired electron orbital by Eq. 1 according to Bleaney et al.,[8]

$$(1/2)\sqrt{5}f(r)(ax^2+by^2+cz^2), \quad (1)$$

with the conditions $a+b+c=0$ and $a^2+b^2+c^2=6$. The wave functions for the $t_{2g}$ orbitals are expressed as

Table 1. EPR Parameters of the trenMe$_6$ and tren Copper Complexes Determined by Simulation of EPR Spectra

| | Compounds | $g_x$ | $g_y$ | $g_z$ | $\lvert^{Cu}A_x\rvert$/MHz | $\lvert^{Cu}A_y\rvert$/MHz | $\lvert^{Cu}A_z\rvert$/MHz |
|---|---|---|---|---|---|---|---|
| **1** | [Cu(trenMe$_6$)ClO$_4$]ClO$_4$ | 2.200 | 2.174 | 1.981 | 340 | 310 | 110 |
| **2** | [Cu(trenMe$_6$)Br]Br | 2.183 | 2.182 | 1.943 | 270 | 325 | 190 |
| **3** | [Cu(trenMe$_6$)I]ClO$_4$[a)] | 2.22 | | 1.88 | 317 | | 296 |
| | | 2.18 | | 1.91 | 344 | | 282 |
| **4** | [Cu(trenMe$_6$)Cl]ClO$_4$ | 2.183 | 2.180 | 2.010 | 240 | 300 | 120 |
| **5** | [Cu(trenMe$_6$)NCS]SCN | 2.189 | 2.174 | 1.995 | 360 | 275 | 150 |
| **6** | [Cu(trenMe$_6$)NH$_3$](ClO$_4$)$_2$ | 2.180 | 2.168 | 1.998 | 321 | 285 | 188 |
| **7** | [Cu(tren)NCS]SCN | 2.207 | 2.168 | 1.990 | 390 | 250 | 165 |
| **8** | [Cu(tren)NH$_3$](ClO$_4$)$_2$ | 2.176 | 2.175 | 1.993 | 280 | 332 | 155 |

a) The parameters were obtained from the spectrum without spectral simulation.

$$\sqrt{15}f(r)yz, \quad \sqrt{15}f(r)zx, \quad \sqrt{15}f(r)xy. \tag{2}$$

The spin-orbit coupling admixes the triplet wave functions with the ground spin orbital and the resultant second-order ground doublet can be written as

$$(1/2)\sqrt{5}Nf(r)\left\{(ax^2+by^2+cz^2+i\gamma xy)\xi+(i\alpha yz-\beta zx)\eta\right\},$$
$$(1/2)\sqrt{5}Nf(r)\left\{(i\alpha yz+\beta zx)\xi+(ax^2+by^2+cz^2-i\gamma xy)\eta\right\}, \tag{3}$$

where $\xi$ and $\eta$ are the two spin functions quantitized along the $z$-direction and $N$ is the normalizing factor, given by

$$N^{-2}=1+(\alpha^2+\beta^2+\gamma^2)/12. \tag{4}$$

For given $a$, $b$ and $c$, the constants $\alpha$, $\beta$, and $\gamma$ can be calculated in terms of the spin-orbit coupling constant ($\lambda$) and $\Delta E_x$, $\Delta E_y$, and $\Delta E_z$, which are the respective energy differences between each $t_{2g}$ orbital and the ground orbital level. By using u, v, and w for $-\lambda/\Delta E_x$, $-\lambda/\Delta E_y$, and $-\lambda/\Delta E_z$ for convenience, the $\alpha$, $\beta$, and $\gamma$ are expressed in the first order in $\lambda$ as

$$\alpha=u(b-c),\ \beta=v(c-a),$$
$$\gamma=w(a-b). \tag{5}$$

By a standard procedure,[10] the expressions for $g$ and $A$ are derived from Eq. 5 as

$$g_x=2+(2/3)\alpha(b-c),$$
$$g_y=2+(2/3)\beta(c-a), \tag{6}$$
$$g_z=2+(2/3)\gamma(a-b),$$

and

$$hA_x/p=-\varkappa+(2/3)\alpha(b-c)+(1/7)(2a^2-4+\gamma c-\beta b),$$
$$hA_y/p=-\varkappa+(2/3)\beta(c-a)+(1/7)(2b^2-4+\alpha a-\gamma c),$$
$$hA_z/p=\varkappa+(2/3)\gamma(a-b)+(1/7)(2c^2-4+\beta b-\alpha a). \tag{7}$$

Here, $p=(\mu_0/2\pi)2g_n\beta\beta_n\langle r^{-3}\rangle_{3d}$. For convenience, the coefficients in the unpaired spin orbital function are expressed by a single parametric angle ($\delta$) as

$$a=\cos\delta+\sqrt{3}\sin\delta,\ b=\cos\delta-\sqrt{3}\sin\delta,\ c=-2\cos\delta. \tag{8}$$

The $\delta$ value of 180° gives the $d_{z^2}$ ground state. In order to examine the rhombicity in the present copper complexes, the changes in the $\delta$ value as well as $g$ and $A$ by an unsymmetrical variation among the equatorial Cu–N bond lengths were calculated by the extended Hückel MO method using a model tbp complex Cu(NH$_3$)$_5$ with bond lengths of Cu–N (axial)=2.06 and 2.39 Å and Cu–N (equatorial)=2.14 Å. The structure of the model complex was taken from the X-ray structural data of [Cu(trenMe$_6$)Br]ClO$_4$.[9] In the calculation one of the equatorial Cu–N bond lengths (on the $x$ axis) was treated as a variable. Figure 3 shows that the $\delta$ value changes sensitively with this variation of the bond length for the range less than 2.8 Å. This changes correspond to the inclusion of the $d_{z^2-y^2}$ or $d_{z^2-x^2}$ component in the $d_{z^2}$ ground state. For a bond length longer than 2.8 Å, the complex has a $d_{z^2-y^2}$ ground state, where the orbital function becomes insensitive to a change in the bond length. Figures 4 and 5 indicate that a sensitive rhombic distortion in the $g$ and $A$ of the tbp complexes may be related to a sensitive change in the unpaired electron orbital function with structural distortion. It should be noted that such a sensitive variation in the unpaired electron orbital function may come from the closeness of the so-called $d_{z^2}$ and $d_{x^2-y^2}$ orbital levels in the tbp copper complexes by balanced axial and equatorial ligand field strengths.

Listed in Table 2 are the nuclear spin-electron spin coupling paramter ($p$), the core polarization parameter ($\varkappa$), and

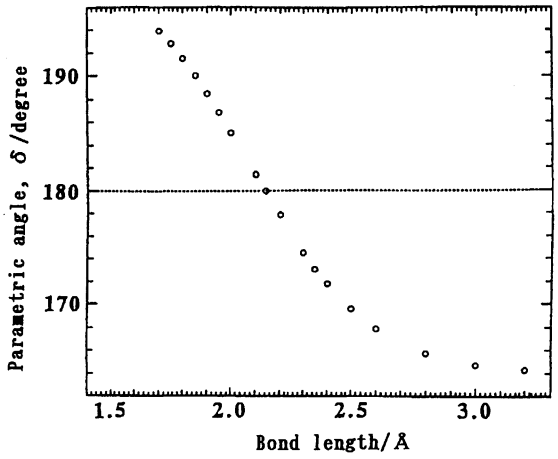


Fig. 3. Change of the parametric angle δ by change of one of the equatorial bond length calculated by the extended Hückel MO method for a model complex.

the d orbital level splitting parameter ($\Delta E$), which were determined by assuming the axial symmetry by taking the average of the experimental $x$- and $y$-direction values. In the calculation a standard value of $\lambda$ of $-828\ cm^{-1}$ (taken from literature[8]) was used. The $\Delta E$ values indicate that the ligand field increases in the order $NH_3 > NCS^- \approx Cl^- > Br^- > ClO_4^-$ and by methyl substitution at the equatorial position. A calculation using Eq. 7 and the parameters given in Table 2 gives negative values for $^{Cu}A_x$ and $^{Cu}A_y$ and a positive value for $^{Cu}A_z$, as shown in Fig. 5. Such different signs for the $^{Cu}A_x$, $^{Cu}A_y$, and $^{Cu}A_z$ were also predicted by Bleaney et al. for some copper complexes.[8] The EPR parameters calculated by Eqs. 6 and 7 are qualitatively consistent with the observed trends of the parameters, though the experimental copper HFC's are more sensitive than the g values to the rhombic distortion and a few cases show that $|^{Cu}A_y| > |^{Cu}A_x|$ for $g_x > g_y$, disagreeing with the calculations.

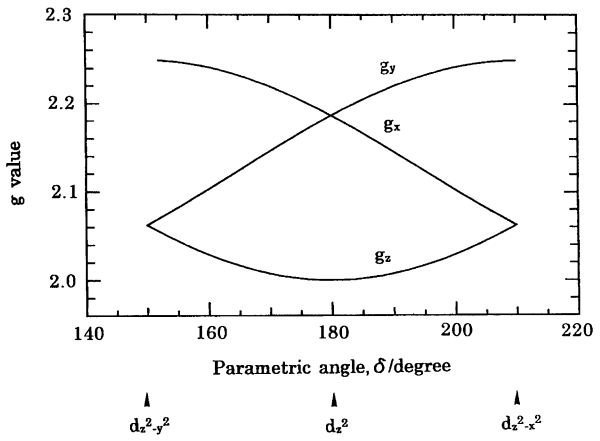


Fig. 4. Changes of $g$ values as a function of the parametric angle $\delta$. The parameters for the complex **1** in Table 2 and $\lambda = -828\ cm^{-1}$ were used for the caluclation.

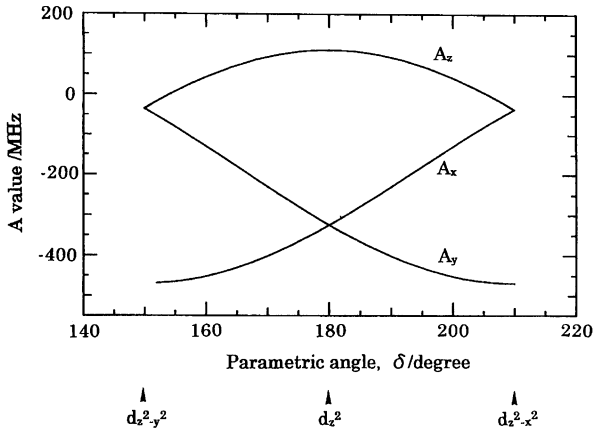


Fig. 5. Changes of copper HFC constants as a function of the parametric angle $\delta$. The parameters used for the calculation are the same as for Fig. 4.

Table 2. Parameters $p$, $\varkappa$, and $\Delta E$

| | Compounds | $p$/MHz | $\varkappa$ | $\Delta E/cm^{-1}$ |
|---|---|---|---|---|
| **1** | $[Cu(trenMe_6)ClO_4]ClO_4$ | 690 | 0.385 | 26600 |
| **2** | $[Cu(trenMe_6)Br]Br$ | 765 | 0.297 | 27300 |
| **4** | $[Cu(trenMe_6)Cl]ClO_4$ | 612 | 0.350 | 27400 |
| **5** | $[Cu(trenMe_6)NCS]SCN$ | 733 | 0.342 | 27400 |
| **6** | $[Cu(trenMe_6)NH_3](ClO_4)_2$ | 760 | 0.299 | 28600 |
| **7** | [Cu(tren)NCS]SCN | 770 | 0.331 | 26500 |
| **8** | $[Cu(tren)NH_3](ClO_4)_2$ | 715 | 0.330 | 28350 |

**Analysis of the ENDOR Spectra.** The ENDOR spectra recorded at different points of EPR for complex **6** are shown in Fig. 6. The ENDOR spectrum taken at point g gives a single-crystal like pattern coming from the molecules, of which the $g_{//}$ axis is oriented parallel to the magnetic field, while the spectra taken at the magnetic field corresponding to the $g_\perp$ region become the so-called powder pattern. The proton and nitrogen ENDOR frequencies were analyzed using the following equations based on a first-order approximation:

$$\nu_H = \nu_{z(H)} \pm {}^{H}A/2, \tag{9}$$

and

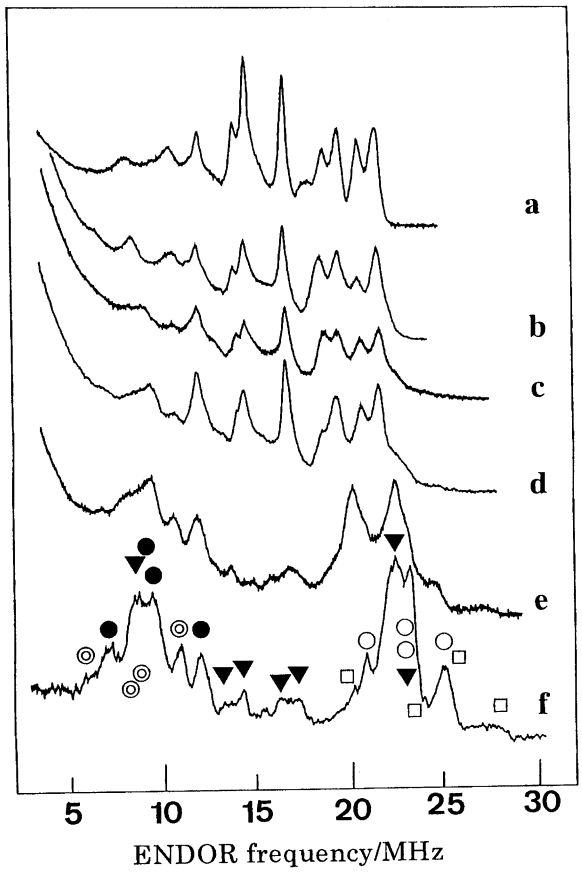


Fig. 6. Powder ENDOR spectra of $[Cu(trenMe_6)NCS]SCN$ recorded at the magnetic field indicated by the corresponding marks a—g in Fig. 2, and at temperature 5—10 K and MW frequency of 9.4109 GHz. The equatorial nitrogen signals are marked with ● and ◎, the axial tbp nitrogen signals with ○, the axial NCS nitrogen signals with □, and the proton signals with ▼, respectively.

$$\nu_N = {}^NA/2 \pm \nu_{z(N)} \pm c. \quad (10)$$

Here, ${}^HA$ and ${}^NA$ represent the proton and nitrogen HFC constants in frequency unit, $\nu_{z(H)}$ and $\nu_{z(N)}$ are the proton and nitrogen nuclear Zeeman frequencies ($g_n\beta_nB/h$), and $c$ stands for the nitrogen nuclear quadrupole splitting (3/2)($Q/h$).

As Fig. 6 shows, although the ENDOR spectra contain many proton signals in addition to the nitrogen signals, for a reliable assignment of the proton signals more elaborate analyses are required than for the analysis of the nitrogen signals. Hence, the following discussion will be focused on the nitrogen ENDOR, which gives more useful and direct information on the metal ligand interaction than the proton ENDOR.

The signals for nitrogens at the equatorial and axial positions were assigned by considering the following points: i) The unpaired electron in the $d_{z^2}$ orbital is expected to distribute along the axial direction in an amount double that of the equatorial direction; hence, the axial nitrogen should have a larger HFC constant than that for the equatorial nitrogens. ii) The hybridized state of the nitrogen appreciably affects the nitrogen HFC; the change in the sp ratio in the nitrogen orbital changes the proportion of isotropic and anisotropic parts in the nitrogen HFC, as well as the magnitudes of the HFC constants, because the unpaired spin in the nitrogen s-orbital gives about a thirty-times greater HFC constant than does the same amount of spin in the nitrogen p-orbital. In cases 5 and 7, the SCN nitrogen is in the sp hybridized state, and, hence, when it is coordinated at the axial position it shows a greater HFC and has a larger isotropic component than do those of the tripodal ligand axial nitrogen. iii) The relative orientation of the HFC tensor to the g tensor must be useful for an assignment. The largest principal value of the nitrogen HFC is usually along to the N–Cu bond direction. Hence, the axial and equatorial nitrogen signals show completely different shifts in measurements of the angle-selected ENDOR in which the spectra are recorded by changing the magnetic field setting position from one side of the EPR spectrum to the other side. iv) The common structural features give common spectral features among the compounds.

In general, the ENDOR spectra taken at the $g_\perp$ region for all of the compounds show two sets of nitrogen signals: one is in the 12—16 MHz region; the other is in the 6—10 MHz region. As the magnetic field setting moves toward the $g_{//}$ region, the former signals move towards higher ENDOR frequencies, and the latter moves towards lower frequencies, indicating that the former HFC principal axis with the largest principal value is directed in the $g_{//}$ direction, while the latter is in the $g_\perp$ direction. For these reasons, the nitrogen signals at 12—15 MHz can be assigned to the nitrogen coordinated at the axial position, while those at 6—8 MHz are assigned to the equatorial nitrogens.

As the ENDOR spectra for **6** in Fig. 6 show, complexes **5**—**8**, with the ligand $NH_3$ or NCS at the fifth position of tbp, give two sets of nitrogen signals at the high-frequency region, one of which can be attributed to the nitrogen donor at the fifth position of tbp.[3] The appearance of the additional nitrogen signals for **5** and **7** is also experimental proof showing that NCS is coordinated to copper by the NCS nitrogen in these complexes.

The X-ray analysis data indicate that in the tren complexes the axial Cu–N bond is longer than the axial Cu–X bond (X=$NH_3$, NCS etc.),[9] whereas in the trenMe$_6$ complexes the axial M–N bond is shorter than the M–Br bond (M=Cu, Co, Ni).[10,11] Such a difference may be caused by a steric effect of the methyl substitution at the equatorial position. As a consequence, the signals for the $NH_3$ nitrogen of **6** are situated at lower frequencies than those of the trenMe$_6$ axial nitrogen, which is opposite to the trend in the tren complexes. As is shown below (Table 5), the spin density is higher on the trenMe$_6$ nitrogen than that on $NH_3$ at the fifth position in the trenMe$_6$ complexes, which may result from such structural features.

As expected form the rhombicity of the EPR spectra, the ENDOR spectra of complexes **5**, **6**, and **7** show signals due to two sets of equatorial nitrogens at the low-frequency region of 6—8 MHz, indicating the presence of some sort of rhombic distortion. In the case of complex **1**, although the equatorial nitrogen signals show some line-width broadening effects they do not show any splitting due to rhombic distortion, in spite that the complex shows a clear rhombic distortion in the $g$ values. In general, when a rhombic distortion in EPR is observed only in copper HF splitting the effects of the rhombicity on ENDOR are either small or negligible. It may be noted that for the tren compound **8** with the fifth ligand $NH_3$ rhombic distortion is limited to the copper HFC in contrast to the case for the trenMe$_6$ complex **6** with the same $NH_3$ ligand at the fifth position, showing an appreciable rhombic distortion in both the $g$ value and copper HFC.

As mentioned above, the principal axis of the nitrogen HFC with the largest principal value is along the Cu–N bond axis. As the coordinating nitrogen HFC tensors are nearly axially symmetric, ${}^NA_{//}$ is usually along the Cu–N bond axis and ${}^NA_\perp$ is perpendicular to the Cu–N bond direction. The parallel and perpendicular components of the HFC and NQC constants for the axial nitrogens can be determined from the ENDOR spectra taken at the extreme of $g_{//}$ and $g_\perp$ regions of the EPR spectrum; they are listed in Table 3. For the equatorial nitrogens the ${}^NA_\perp$ values can be read from the ENDOR spectra taken in the $g_{//}$ region, while the ${}^NA_{//}$ values are to be obtained from the spectra taken in the $g_\perp$ region. However, it was difficult to read them from the spectra because the nitrogen signals showed a powder-type pattern, and the parallel component did not have a sufficient signal intensity to read correctly. Table 4 lists only the ${}^NA_\perp$ values.

**Spin Distribution on the Coordinating Nitrogen Atoms.** The HF interactions of the coordinating nitrogens consist of three contribution. One is isotropic coupling due to an unpaired electron delocalized onto the nitrogen 2s orbital; the second and third are the anisotropic couplings due to the spin delocalized onto the nitrogen 2p orbitals and the spin on the copper unpaired electron orbital. The largest contribution to the nitrogen HFC values comes from the isotropic interaction. Assigning the $z$-axis to the Cu–N bond

Table 3. HFC, NQC, and $e^2qQ$ Values for Axial Nitrogens

| | Compounds | ${}^{N}A_{//}$/MHz | $c_{//}$/MHz | ${}^{N}A_{\perp}$/MHz | $c_{\perp}$/MHz | $e^2qQ/h$/MHz |
|---|---|---|---|---|---|---|
| **1** | $[Cu(trenMe_6)ClO_4]ClO_4$ | 49.38 | 2.20 | 29.12 | 1.15 | 2.93 |
| **2** | $[Cu(trenMe_6)Br]Br$ | 44.74 | 2.37 | 26.32 | 1.18 | 3.16 |
| **3** | $[Cu(trenMe_6)I]ClO_4$ | 44.51 | 2.35 | 26.11 | 1.24 | 3.13 |
| **4** | $[Cu(trenMe_6)Cl]ClO_4$ | 42.88 | 2.45 | 25.34 | 1.21 | 3.27 |
| **5** | $[Cu(trenMe_6)NCS]SCN$ | 42.58 | 1.70 | 26.80 | 1.25 | 2.27 |
| | | 49.79[a] | 0.98 | 37.56[a] | 0.43 | 1.30 |
| **6** | $[Cu(trenMe_6)NH_3](ClO_4)_2$ | 42.52 | 2.47 | 25.20 | 1.39 | 3.29 |
| | | 35.01[b] | 1.46 | 24.24[a] | 0.54 | 1.95 |
| **7** | $[Cu(tren)NCS]SCN$ | 42.30 | 1.70 | 28.30 | 1.20 | 1.94 |
| | | 49.90[a] | 1.00 | 44.00[a] | 0.40 | 1.98 |
| **8** | $[Cu(tren)NH_3](ClO_4)_2$ | 41.50 | 1.80 | 27.90 | 1.27 | 1.40 |
| | | 44.70[b] | 1.36 | 30.68[b] | 0.90 | 2.44 |

a) and b) are the values for $NH_3$ and NCS nitrogens, respectively.

Table 4. Perpendicular Components of HFC and NQC for Equatorial Nitrogens

| | Compounds | ${}^{N}A_{\perp}$/MHz | $c_{\perp}$/MHz | $\rho(2s)$ | $\rho_{equatorial}$ |
|---|---|---|---|---|---|
| **1** | $[Cu(trenMe_6)ClO_4]ClO_4$ | 14.48 | 1.27 | 0.0104 | 0.0416 |
| **2** | $[Cu(trenMe_6)Br]Br$ | 14.80 | 1.26 | 0.0106 | 0.0424 |
| **3** | $[Cu(trenMe_6)I]ClO_4$ | 15.30 | 1.26 | 0.0101 | 0.0404 |
| **4** | $[Cu(trenMe_6)Cl]ClO_4$ | 15.52 | 1.37 | 0.0111 | 0.0444 |
| **5** | $[Cu(trenMe_6)NCS]SCN$ | 15.90 | 1.29 | 0.0114 | 0.0456 |
| | | 18.10 | 1.25 | 0.0129 | 0.0516 |
| **6** | $[Cu(trenMe_6)NH_3](ClO_4)_2$ | 16.49 | 1.31 | 0.0118 | 0.0472 |
| | | 14.54 | 1.41 | 0.0104 | 0.0416 |
| **7** | $[Cu(tren)NCS]SCN$ | 16.24 | 1.89 | 0.0116 | 0.0464 |
| | | 18.90 | 2.48 | 0.0135 | 0.0540 |
| **8** | $[Cu(tren)NH_3](ClO_4)_2$ | 13.50 | 1.45 | 0.0098 | 0.0392 |

Table 5. Isotropic and Anisotropic HFC Constants and Spin Densities of Axial Nitrogens

| | Compounds | ${}^{N}A_{iso}$/MHz | ${}^{N}A_{aniso}$/MHz | $\rho(2s)$ | $\rho(2p_z)$ | $\rho(2p_z)/\rho(2s)$ | $\rho(2p_z)+\rho(2s)$ $=\rho_{axial}$ |
|---|---|---|---|---|---|---|---|
| **1** | $[Cu(trenMe_6)ClO_4]ClO_4$ | 35.87 | 13.51 | 0.0232 | 0.141 | 6.09 | 0.165 |
| **2** | $[Cu(trenMe_6)Br]Br$ | 32.46 | 12.28 | 0.0211 | 0.129 | 6.09 | 0.150 |
| **3** | $[Cu(trenMe_6)I]ClO_4$ | 32.24 | 12.27 | 0.0209 | 0.128 | 6.13 | 0.149 |
| **4** | $[Cu(trenMe_6)Cl]ClO_4$ | 31.19 | 11.69 | 0.0202 | 0.122 | 6.05 | 0.142 |
| **5** | $[Cu(trenMe_6)NCS]SCN$ | 32.23 | 10.85 | 0.0209 | 0.114 | 5.43 | 0.134 |
| | | 39.31 | 3.49 | 0.0255 | 0.037 | 1.43 | 0.062 |
| **6** | $[Cu(trenMe_6)NH_3](ClO_4)_2$ | 30.97 | 11.55 | 0.0201 | 0.121 | 6.00 | 0.141 |
| | | 27.83 | 7.17 | 0.0181 | 0.075 | 4.14 | 0.093 |
| **7** | $[Cu(tren)NCS]SCN$ | 33.53 | 10.51 | 0.0218 | 0.110 | 5.04 | 0.132 |
| | | 45.96 | 3.94 | 0.0298 | 0.041 | 1.38 | 0.071 |
| **8** | $[Cu(tren)NH_3](ClO_4)_2$ | 33.14 | 10.49 | 0.0215 | 0.110 | 5.10 | 0.131 |
| | | 35.35 | 9.43 | 0.0229 | 0.099 | 4.31 | 0.122 |

direction, as a local coordinate, the principal values of HFC are expressed as:

$$\begin{aligned} {}^{N}A_{xx} &= \rho_{2s}{}^{N}A_{2s} - \rho_{2p}{}^{N}A_{2p} + {}^{N}A_{dxx}, \\ {}^{N}A_{yy} &= \rho_{2s}{}^{N}A_{2s} - \rho_{2p}{}^{N}A_{2p} + {}^{N}A_{dyy}, \\ {}^{N}A_{zz} &= \rho_{2s}{}^{N}A_{2s} + \rho_{2p}{}^{N}A_{2p} + {}^{N}A_{dzz}. \end{aligned} \quad (11)$$

Here, ${}^{N}A_{2s}$ is isotropic coupling resulting from the interaction of the single electron spin distributing on the nitrogen 2s orbital, ${}^{N}A_{2p}$ stands for dipolar coupling with the single electron spin on the nitrogen 2p orbital and ${}^{N}A_{dii}$ is the dipolar interaction with spin on the metal unpaired electron orbital. Since ${}^{N}A_{dii}$ have values of about 0.9 MHz in absolute value, and they are much smaller than the total magnitude of nitrogen HFC, the HFC tensors become nearly axially symmetric. Hence, in the following, the contribution of ${}^{N}A_{dii}$ is ignored. By assigning the values 1540 and 47.8 MHz to ${}^{N}A_{2s}$ and ${}^{N}A_{2p}$, respectively,[12] the unpaired electron population on the nitrogen 2s and 2p orbitals of the coordinating nitrogens can be obtained by Eq. 11. The obtained spin densities for the axial nitrogens are listed in Table 5. For the equatorial nitrogens, for which the ${}^{N}A_{//}$ values have not been

determined, we assumed $\rho_{2p}=3\rho_{2s}$ under the assumption of $sp^3$ hybridization. Hence, the isotropic spin densities on the equatorial nitrogens are estimated from ${}^{N}A_{\perp}$ by Eq. 12, and the total spin densities are given for the equatorial nitrogens by $\rho(\text{eq})\fallingdotseq 4\rho_{2s}(\text{eq})$. They are tabulated in Table 4.

$$\rho_{2s} = {}^{N}A_{+}/\left({}^{N}A_{2s} - 3{}^{N}A_{2p}\right) \quad (12)$$

**Effects of the Fifth Ligand and Methyl Substitution at the Equatorial Nitrogen on the Spin Distribution.** In the complexes of tren and trenMe$_6$, different ligands can be substituted at the fifth position. These ligands affect the spin distribution on the whole molecule; this affects all of the copper-ligand bondings. Tables 4 and 5 show that the spin density on the axial nitrogen decreases, and that of the equatorial nitrogens increases by the ligand in the order of increasing ligand field strength, which are shown by $\Delta E$ values in the EPR analysis. Exceptions are the axial nitrogens for **5** and **6** and the equatorial nitrogens for **7** and **8**. The methyl substitution at the $NH_2$ protons of tren also affects the spin distribution; an increase of the ligand field strength due to methyl substitution makes the spin density at the axial nitrogen larger.

The trends in the changes of the spin distribution can be explained by the changes in the mixing of the copper unpaired electron orbital among $3d_{z^2}$, 4s, and 4p by the ligand field strength. With increasing ligand field at the fifth position, the 4s and $4p_z$ orbitals mix with the $3d_{z^2}$ orbital, so that the orbital lobe at the fifth ligand position shrinks. The mixing with the 4s orbital with negative sign causes a shrinking of the orbital lobe at the direction to the tren nitrogen, and a simultaneous expansion of the lobe at the equatorial direction. On the other hand, the mixing with the 4p orbital causes an expansion of the orbital lobe towards the tren nitrogen in contrast to the effect of mixing of the 4s orbital. Such effects of the orbital mixing are schematically drawn in Fig. 7. The observed decrease in HFC of the tren nitrogen with increasing ligand field at the fifth position indicates that the effect of the 4s orbital mixing overwhelms the effect of the 4p orbital mixing, probably due to the lower energy level of the 4s orbital. On the other hand, when the ligand field at the equatorial positions increases as in the methyl substitution at the equatorial $NH_2$ protons, the 4s orbital mixes with the $3d_{z^2}$ orbital in an opposite sign to the above case, so that the lobe of the unpaired electron orbital along the equatorial plane becomes smaller and that of the axial direction expands.

**Examination of the Ligand Field Effects on the Spin Distribution by the MO Calculation.** The ligand field effects on the spin distribution presented above were confirmed by an extended Hückel MO calculation using the model compound shown in Fig. 8. In the calculation, the variation in the ligand field strength was given by changing the axial or equatorial Cu–N bond length ($r_1$,$r_2$, or $r_3$), or by putting a different halogen at the fifth coordination position (X). Some results of the calculation are shown in Fig. 9. In the calculation of Fig. 9, $r_1$ and $r_3$ are taken to be 2.06 and 2.14 Å, respectively, and the axial ligand field is changed by

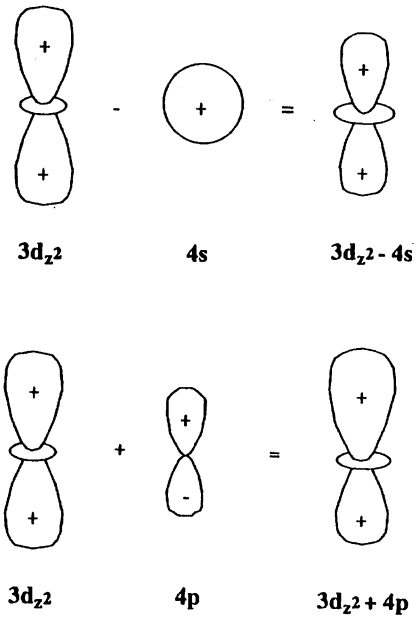


Fig. 7. Schematic drawing for the effects of the orbital mixing.

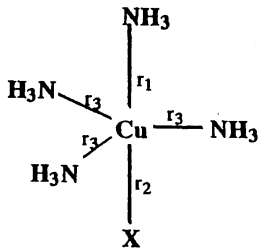


Fig. 8. A model complex used for the MO calculation.

changing the bond length $r_2$ from 2.06 to 2.39 Å or/and by a different halogen. In the figure the axial ligand fields are expressed as a function of the $d_{z^2}$ orbital level; the increase in the $d_{z^2}$ orbital level corresponds to the increase in the ligand field strength by shortening of the Cu–N bond length or by changing X in the order of $I^-$, $Br^-$, and $Cl^-$.

Figure 9 shows that the spin densities on the 2s and 2p orbitals of the axial nitrogen (at the top position) decrease along with an increase in the axial ligand field at the fifth (botton) position (Fig. 9a), while the spin densities on the 2s and 2p orbitals of the equatorial nitrogens exhibit the opposite trend (Fig. 9b). Such changes of the spin distribution on the axial and equatrial nitrogens are related to the orbital mixing on the copper ion, as shown in Fig. 9c. In this model the copper $3d_{z^2}$ orbital is mixed with the copper 4s and 4p orbitals, the former orbital function having a positive or a negative sign, depending on the axial ligand field strength and the latter function having a negative sign, reflecting the weaker ligand field at the fifth position due to the longer Cu–N bond length than that from the axial ligand at the top. Increasing the ligand field at the fifth position causes a decrease in the mixing of the 4p orbital with a negative sign, and also leads to a mixing of the negative copper 4s function. These results are well consistent with those discussed above.

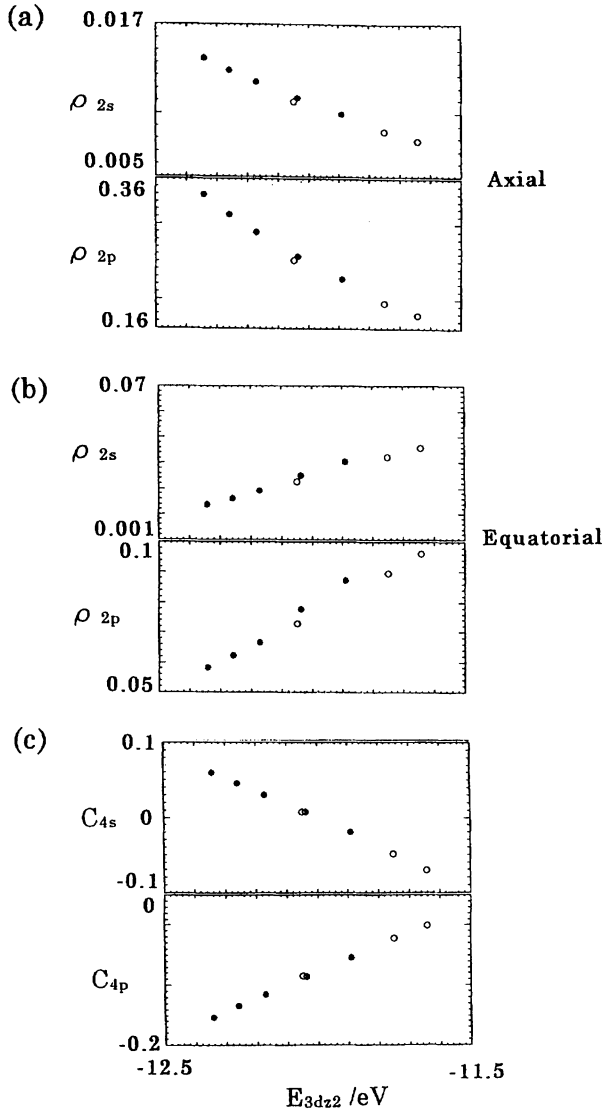


Fig. 9. Changes of spin densities on 2s and 2p orbitals of (a) axial and (b) equatorial nitrogens and (c) changes of copper 4s and 4p orbital function coefficients with increases of the ligand field strength at the fifth (botton) position, expressed as a function of the $3d_{z^2}$ orbital level. The open circles are for X=$NH_3$ and the closed circles are for X=halogen in the model complex.

**The sp Ratio of the Coordinating Nitrogen Orbitals.** In complexes **5**—**8**, the anisotropies of the HFC for the two axial nitrogens, $NH_3$ and NCS, are largely different from each other: the former is more anisotropic than the latter. The $\rho(2p)/\rho(2s)$ ratios, determined from the ENDOR analysis (4.15 (**6**) and 4.31 (**8**) for the $NH_3$ nitrogens and 1.43 (**5**) and 1.38 (**7**) for the NCS nitrogen) well reflect the difference in the hybridized states of the $NH_3$ and NCS nitrogens; the former is close to the $sp^3$ hybridized state and the latter to the sp state.

For all compounds the $\rho(2p)/\rho(2s)$ ratios of the axial nitrogens of the tripodal ligands are greater than those of the regular $sp^3$ hybridized nitrogen. This suggests a distortion of the Cu–N–C bond angles due to coordination. For an $sp^3$ hybridized nitrogen, the standard orbital functions can be written as

$$\phi_1 = \sqrt{\frac{-\cos\alpha}{1-\cos\alpha}}\varphi_s - \sqrt{\frac{2}{3}}\varphi_x + \sqrt{\frac{1+2\cos\alpha}{3(1-\cos\alpha)}}\varphi_z,$$

$$\phi_2 = \sqrt{\frac{-\cos\alpha}{1-\cos\alpha}}\varphi_s - \sqrt{\frac{1}{6}}\varphi_x + \frac{1}{\sqrt{2}}\varphi_y + \sqrt{\frac{1+2\cos\alpha}{3(1-\cos\alpha)}}\varphi_z,$$

$$\phi_3 = \sqrt{\frac{-\cos\alpha}{1-\cos\alpha}}\varphi_s + \sqrt{\frac{1}{6}}\varphi_x - \frac{1}{\sqrt{2}}\varphi_y + \sqrt{\frac{1+2\cos\alpha}{3(1-\cos\alpha)}}\varphi_z,$$

$$\phi_4 = \sqrt{\frac{1+2\cos\alpha}{1-\cos\alpha}}\varphi_s - \sqrt{\frac{-3\cos\alpha}{1-\cos\alpha}}\varphi_z. \quad (13)$$

Here, $\alpha$ is the C–N–C tetrahedral angle, and $\phi_4$ is the lone-pair orbital containing two electrons. The angle $\alpha$ is related to the Cu–N–C bond angle ($\theta$) by Eq. 14 for the Cu–N–$C_3$ system with a $C_3$ symmetry,

$$\cos\alpha = 1 - \frac{3}{2}\sin^2\theta. \quad (14)$$

Hence, the $\rho(2p)/\rho(2s)$ ratio is expressed as a function of $\theta$ as

$$\frac{\rho(2p)}{\rho(2s)} = \frac{-(1+3\cos 2\theta)}{2(\cos 2\theta + 1)}. \quad (15)$$

This equation shows that the $\rho(2p)/\rho(2s)$ ratio changes sensitively with $\theta$. The $\rho(2p)/\rho(2s)$ ratios estimated from the ENDOR data indicate that the complexes undergo a distortion of 3—4° in the Cu–N–C angle from the normal tetrahedral angle of 109°28′. This estimation is consistent with the Cu–N–C bond angles, 106.9° and 108°, for the tren complexes (**7** and **8**) determined by an X-ray analysis.[13]

**Total Spin Distribution on Coordinating Nitrogens.** In the case of tetragonal or tetragonal pyramidal copper complexes, the unpaired electron is usually in the $d_{x^2-y^2}$ orbital on the tetragonal plane. In these cases, even when the copper is coordinated by a nitrogen base at the axial position of the tetragonal plane, the ENDOR rarely observes the coordinating axial nitrogen. In the present case, the ENDOR signals due to all of the coordinating nitrogens were observed for complexes **5**—**8**. As a consequence, the total spin densities distributed among all of the coordinating atoms could be determined. Table 6 shows that the delocalized spin on the coordinating atoms amounts to about 36%. This is larger than the spin distribution in ligands in ordinary tetragonal copper complexes with nitrogen donor ligands, which is usually considered to be about 20—30%. It may be also notable that the total spin densities on the coordinating nitrogens in the $trenMe_6$ compounds are less than those in the corresponding tren compounds.

**Nuclear Quadrupole Interaction.** By using Eq. 13, we can derive Eq. 16 for the quadrupole couplings according to the Townes and Dailey analysis,[14]

$$\frac{e^2qQ}{e^2qQ_0} = -\frac{3\cos\alpha}{1-\cos\alpha}(b-a), \quad (16)$$

where $b$ is the electron population in the nitrogen lone-pair orbital and $a$ is the electron population on nitrogen in the sigma bond. This equation indicates that the nuclear

Table 6. Spin Distribution on the Coordinating Nitrogen Atoms

| | Compounds | $\rho_{axial}$ [a)] | | $\rho_{equatorial}$ | $\rho_{total}$ [a)] |
|---|---|---|---|---|---|
| **1** | $[Cu(trenMe_6)ClO_4]ClO_4$ | 0.150 | | 0.125 | 0.275 |
| **2** | $[Cu(trenMe_6)Br]Br$ | 0.150 | | 0.127 | 0.277 |
| **3** | $[Cu(trenMe_6)I]ClO_4$ | 0.147 | | 0.131 | 0.278 |
| **4** | $[Cu(trenMe_6)Cl]ClO_4$ | 0.142 | | 0.133 | 0.275 |
| **5** | $[Cu(trenMe_6)NCS]SCN$ | 0.134 | (0.196) | 0.146 | 0.280 (0.342) |
| **6** | $[Cu(trenMe_6)NH_3](ClO_4)_2$ | 0.141 | (0.234) | 0.133 | 0.274 (0.367) |
| **7** | $[Cu(tren)NCS]SCN$ | 0.132 | (0.203) | 0.151 | 0.281 (0.353) |
| **8** | $[Cu(tren)NH_3](ClO_4)_2$ | 0.131 | (0.253) | 0.118 | 0.249 (0.370) |

a) The numbers in the parentheses are the total spin densities including the spin on the $NH_3$ or NCS nitrogen.

quadrupole coupling constant is proportional to parameter $a$ and $(3\cos\alpha)/(1-\cos\alpha)$. It is indicated above that the axial nitrogens are distorted from the ordinary $sp^3$ hybridized state. This angular distortion also affects the $e^2qQ$ values. However, the obtained $\rho(2p)/\rho(2s)$ ratios indicate that the angular distortion is more or less the same for all complexes. Hence, we can assume that the effect of distortion on the $e^2qQ$ is nearly the same for all compounds, and, hence, the $e^2qQ$ value may be expected to be proportional to $a$ in the present system. Table 3 shows that the value of $e^2qQ$ increases with the ligand field strength at the fifth position. They correlate well to the nature of the Cu–N bondings; the increase of covalency with copper makes the $e^2qQ$ value greater.

As a conclusive remark, one can say that the characteristic features of the tbp copper complexes have been clarified by EPR and ENDOR studies concerning complexes of the quadridentate tripodal nitrogen donor ligands with different ligands at the fifth position of tbp.

We acknowledge the financial support by Grants-in-Aid of Scientific Research Nos. 02453036 and 06640711 from the Ministry of Education, Science and Culture.

## References

1) a) G. H. Rist and J. S. Hyde, *J. Chem. Phys.*, **50**, 4532 (1969); b) G. H. Rist and J. S. Hyde, *J. Chem. Phys.*, **52**, 4633 (1970); c) B. M. Hoffman, J. Martinsen, and R. A. Venters, *J. Magn. Reson.*, **59**, 110 (1984); d) N. D. Yordanov and M. Zdravkov, in "XXIInd Congress Ampere on Magnetic Resonance and Related Phenomena Proceedings," Zurich, 1984, Abstr., p. 612; e) T. A. Henderson, G. C. Hurst, and R. W. Krelick, *J. Am. Chem. Soc.*, **107**, 7299 (1985); f) N. D. Yordanov and M. Zdrakova, *Acta Phys. Hung.*, **61**, 127 (1987); g) J. Stach, R. Kirmse, U. Abram, R. Bottcher, J. Sieler, W. Dietzsh, L. K. Hansen, H. Vergoossen, M. C. M. Gribnau, and C. P. Keijzers, *Inorg. Chem.*, **25**, 1369 (1986); h) M. Iwaizumi, T. Kudo, and S. Kita, *Inorg. Chem.*, **25**, 1546 (1986); i) R. Miyamoto, Y. Ohba, and M. Iwaizumi, "Electron Magnetic Resonance of Disordered System," ed by N. D. Yordanov, World Scientific, (1989), p. 113; j) R. Miyamoto, Y. Ohba, and M. Iwaizumi, *Inorg. Chem.*, **29**, 3234 (1990); k) R. Miyamoto, Y. Ohba, and M. Iwaizumi, *Inorg. Chem.*, **31**, 3138 (1992).

2) a) W. B. Mims, *J. Biochem.*, **15**, 3863 (1976); b) J. E. Roberts, T. G. Brown, B. M. Hoffman, and J. Peisach, *J. Am. Chem. Soc.*, **102**, 825 (1980); c) J. E. Roberts, J. F. Cline, V. Lum, H. Freeman, H. B. Gray, J. Peisach, B. Reinhammar, and B. M. Hoffman, *J. Am. Chem. Soc.*, **106**, 5324 (1984); d) M. M. Werst, C. E. Davoust, and B. M. Hoffman, *J. Am. Chem. Soc.*, **113**, 1533 (1991).

3) M. Q. Ehsan, Y. Ohba, S. Yamauchi, and M. Iwaizumi, *Chem. Lett.*, **1995**, 151.

4) F. Jiang, K. D. Karlin, and J. Peisach, *Inorg. Chem.*, **32**, 2576 (1993).

5) R. N. Icke and B. B. Wiesegarver, *Org. Synth.*, **3**, 723 (1955).

6) a) R. Barbucci and M. J. M. Cambell, *Inorg. Chim. Acta.*, **15**, L15 (1975); b) B. J. Hathaway, D. E. Billing, R. J. Dudley, R. J. Faraday, and A. G. Tomlinson, *J. Chem. Soc. A*, **1970**, 806; c) G. A. Senyukova, I. D. Mikheikin, and K. I. Zamaraev, *J. Struct. Chem.* (*Engl. Transl.*), **11**, 18 (1970).

7) M. Iwasaki, *J. Magn. Reson.*, **16**, 417 (1974).

8) B. Bleaney, K. D. Bowers, and M. H. L. Pryce, *Proc. R. Soc. London, Ser. A*, **228A**, 166 (1955).

9) M. D. Viria and P. L. Orioli, *Acta Crystallogr., Sect. B*, **B24**, 595 (1968).

10) M. D. Viria and P. L. Orioli, *Inorg. Chem.*, **6**, 955 (1967).

11) M. Dugan, N. Ray, B. Hathaway, G. Tomlinson, P. Brint, and K. Pelin, *J. Chem. Soc., Dalton Trans.*, **1980**, 1342.

12) J. E. Wertz and J. R. Bolton, "Electron Spin Resonance," McGraw-Hill Book Company, New York (1972).

13) M. Dugan, N. Ray, B. Hathaway, G. Tomlinson, P. Brint, and K. Pelin, *J. Chem. Soc., Dalton Trans.*, **1980**, 1342.

14) C. H. Townes and B. P. Dailey, *J. Chem. Phys.*, **17**, 782 (1949).